

Dynamics of salt marsh margins are related to their 3-dimensional functional form

Evans, B.R.; Möller, I.; Spencer, T.; Smith, G.

March 6, 2019

Abstract

The three-dimensional configuration of sedimentary landforms in intertidal environments represents a major control on regional hydrodynamics. It modulates the location and magnitude of forces exerted by tidal currents and waves on the landform itself and on engineered infrastructure such as sea walls or coastal defences. Furthermore, the effect is reflexive with the landforms representing an integrated, long-term response to the forces exerted on them. There is a strong reciprocal linkage between form and process (morphodynamics) in the coastal zone which is significantly lagged and poorly understood in the case of cohesive, vegetated sediments in the intertidal zone. A method is presented that links the geometric properties of the tidal flat-saltmarsh interface to the history and potential future evolution of that interface. A novel quantitative classification scheme that is capable of separating marsh margins based on their functional form is developed and is applied to demonstrate that relationships exist between landform configuration and morphological evolution across a regional extent. This provides evidence of a spatially variable balance between self-organised and external controls on morphodynamic evolution and the first quantitative basis for a quick assessment procedure for likely future dynamism.

1 Introduction

The strong feedbacks between sedimentary and hydrodynamic systems in the intertidal zone have been widely documented (Defina et al., 2007; Fagherazzi et al., 2004; van de Koppel et al., 2012) and highlight the

18 dynamic and highly functional nature of the topography within such systems. The characteristics of intertidal
19 landforms have the potential to provide information both on the modification of hydrodynamic forces caused
20 by the landform but also the process history at the location (unless this has been 'overwritten' by the
21 effects of a high magnitude event (Cahoon, 2006)). Under an assumption of stationarity in the relationship
22 between form and process, landforms perhaps also contain an indication of the 'process future', since their
23 current configuration may be predictive of their ongoing geomorphic interaction with the hydrodynamic
24 environment. At the large scale, as demonstrated here, marginal morphometry could have wider applications
25 as a means of measuring landscape heterogeneity and micro-habitat or niche provision, in the study of
26 ecosystem functioning and ecosystem service delivery over large areas.

27 Attempts have been made to categorise types of mudflat in conceptual (Dyer, 1998) and quantitative
28 (Townend (2008); Dyer et al. (2000)) terms. No formal *functional* typology for vegetated upper tidal flat
29 (saltmarsh) margins, analogous to the work of Dyer (1998) and Dyer et al. (2000) on mudflats, appears to have
30 been attempted to date. Similarly, no quantitative descriptions of contrasting marsh margin configurations
31 are currently available. When considering different landform configurations at the interface between the
32 vegetated marsh and the fronting foreshore, discussions tend to be dominated by ideas of cross-shore slope
33 and whether there is a cliff or scarp present. Allen (2000) discusses in a more explicit manner some of the
34 differences between cliffed and ramped margins. He presents a genetic typology dividing ramped margins
35 into three classes of origin but does not discuss their real-time functions within the system.

36 Explicit, quantitative landform descriptors are essential as a baseline measurement against which future
37 three-dimensional changes in functional form may be assessed and predictions from morphological models
38 may be validated. Quantitative description of landform characteristics also increases the variety and power
39 of statistical methods available to investigate the nature of the interactions that occur at marsh margins
40 (between hydrodynamics and sediment erosion, transport and deposition), their relative importance, effects
41 and spatial distribution.

42 Fundamentally, the marsh margin represents the transition from an area too low in the tidal frame for
43 vegetation to develop to an area high enough to be perennially vegetated. Within intertidal environments
44 elevation exerts a primary control on vegetation establishment (Morris et al., 2002; Suchrow and Jensen,

45 2010; Marani et al., 2013; Roner et al., 2016). The vegetated margin therefore represents the spatial location
46 of a critical elevation within the more general cross-shore slope.

47 A spectrum of margin slopes exists from gentle ramps extending tens of metres in the cross-shore to
48 vertical scarps or cliffs where the cross-shore extent might be sub-metre (Allen, 1993). In addition to this
49 variation a range of smaller-scale (metre or centimetre) topographic characteristics may be superimposed
50 upon the general marginal slope (both along- and across-shore). These may include linear or non-linear
51 topographic features creating sub-margin scale variations in elevation, slope and aspect. For cliffed cases,
52 variations in planform complexity affect the range of orientations observed. In North West Europe, under
53 conditions of moderate sea level rise characteristic of the late Holocene, marshes tend to develop such that
54 the permanently vegetated marsh platform establishes a dynamic equilibrium close to the mean high water
55 spring (MHWS) level (Allen, 1989) while inundation stress (Balke et al., 2016) or exposure (Gray et al.,
56 1989) are too great for vegetation to survive much below mean high water neaps (MHWN). The consequence
57 is that the marginal zone experiences regular inundation and a large variability in inundation depth; there
58 is therefore likely to be a large variance in hydrodynamic conditions leading to diversity in the processes
59 by which the landform affects hydrodynamics and vice versa. As a consequence Allen (2000) argues that
60 the elevation range that characterises the vegetated margin is that in which erosional processes will be most
61 prevalent.

62 To investigate the effects of morphodynamic interactions on landform evolution at landscape and decadal
63 scales it is necessary to parametrise the manifestations of such interactions. To this end, broad categorisation
64 of margin type is helpful if categories can be designed such that they separate different dominant processes,
65 or dominant scales at which processes operate (which may be expected to lead to different system responses
66 through time).

67 This study presents a conceptual typology for marginal landforms, the characteristics and functional
68 influences of which are described. The potential for landform interaction with system processes is out-
69 lined. Morphometric methods are then developed that capture relevant landform attributes and result in a
70 novel, quantitative, functional typology. Marginal form is then compared to observations of decadal-scale
71 morphodynamics and instantaneous-scale hydrodynamic influences. The method also extends possibilities

72 for studies investigating, for example, relationships between marsh edge habitats, faunal assemblages and
73 ecosystem service provision by providing a quantitative description of a major structural component of the
74 habitat that may support the development of niche models (e.g. Whaley and Minello (2002); Minello et al.
75 (1994); Baltz et al. (1993); Glancy et al. (2003)).

76 **1.1 Conceptual functional typology**

77 A classification of marsh margins into three categories is adopted within this study, based on the consideration
78 of three distinct process environments associated with their marginal geometries. There has been little
79 attention given to the relationship between margin geometry and evolutionary tendencies, with this literature
80 hitherto limited to modelling of marsh cliff formation and subsequent erosion (van De Koppel et al., 2005;
81 Singh Chauhan, 2009). Both diversification and validation would therefore be desirable additions to the
82 debate.

83 The three margin types (ramps, cliffs and ridge-runnel) identified by Allen (1993) are adopted by this
84 study. These are represented schematically with photographic examples in Figure 1. The different end-
85 member landforms identified above can be expected to modify and respond to local hydrodynamic conditions
86 in differing ways which in turn will affect their morphological evolution. The landform interactions with
87 hydrodynamics operate at an instantaneous timescale while measurable morphological evolution can only be
88 considered at decadal timescales. This disjuncture is challenging but the morphometric approach used here
89 supposes that between-class differences in the nature of instantaneous interactions, additively realised over
90 decades, will produce measurably different morphological trajectories. The principal landform attributes
91 that may describe instantaneous interactions are cross-shore slope, landform alignment and topographic
92 complexity. For the purposes of this study, 'landform alignment' is used to refer to the relative dominance
93 of slope directions between those that are shore-aligned and those that are shore-normal, at the scale of
94 landforms spanning a number of 25cm pixels. 'Topographic complexity' is used to refer to the magnitude
95 and frequency of elevational changes, again at a scale that can be evaluated with a pixel size of 25cm.

96 Ramped margins have a shallow slope and are therefore the most spatially extensive transition between
97 marsh and tidal flat but with little or no sub-margin scale topographic variation. Characterised by gradual

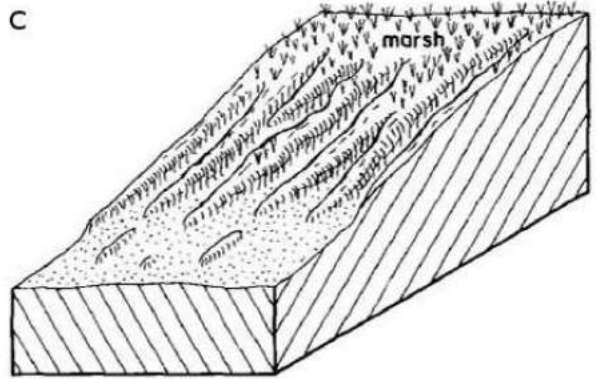
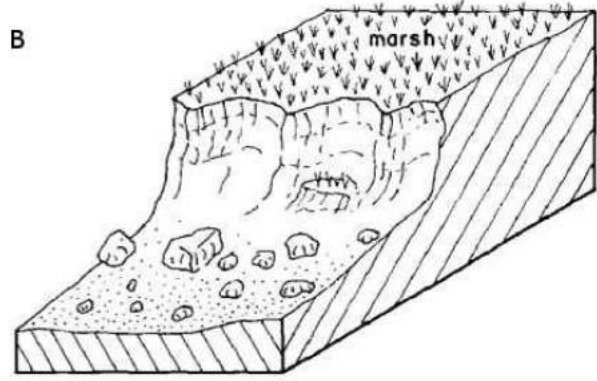
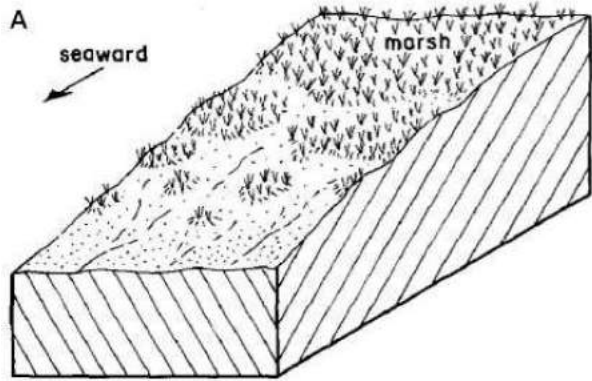


Figure 1: Margin types identified as common within the UK. (A) ramped transition with patchy vegetation (Donna Nook, Lincolnshire). (B) marsh cliff (Abbotts Hall, Essex). (C) ridge-runnel (Tillingham, Essex). Schematics adapted from Allen (1993). Photograph credit: A - Ben Evans, B and C - James Tempest

98 changes in elevation, ramps are highly dissipative features likely to result in the lowest maximum shear
99 stresses being experienced at the sediment surface of any of the landform types. Current flows are likely to
100 be relatively uniform and two-dimensional. Refraction and wave energy attenuation may also be uniform.
101 Sediment mobilisation again depends on shear stress, which is related to the wave height to water depth
102 ratio. If energy is low or sediment loads high and deposition occurs there are limited factors that might
103 lead to preferential accretion in particular locations. Once vegetation or biofilms become established and the
104 feedbacks associated with those developments begin to have an effect, the fine-scale (metres) topographic
105 variability tends to increase (e.g. Temmerman et al., 2007). Given the difficulty in finding vegetated margin
106 zones conforming to a true planar slope this class is more realistically represented by a morphology with
107 some degree of low-amplitude topographic variability superimposed on the underlying cross-shore slope (See
108 Figure 1).

109 Cliffs are the most abrupt and shoreline-aligned marginal transition, being characterised by a scarp,
110 which may exceed 1m in height (e.g. Leonardi and Fagherazzi, 2014). These tend to act as reflectors of wave
111 energy while the water level is between the base and top of the cliff. In the absence of an armouring effect
112 from the persistence of blocks produced by earlier marsh edge failure (Gabet, 1998), the result is the greatest
113 concentration of wave energy of any of the margin types and therefore an increased probability of exceeding
114 the critical shear strength and mobilisation of sediment. Tonelli et al. (2010) find that forces exerted by
115 waves are higher for vertical cliffs than for terraced ones. The vertical faces of cliffs do not tend to allow
116 the establishment of vegetation or other biofilms to increase the stability of the sediment (van De Koppel
117 et al., 2005). They are thus expected to be particularly vulnerable to erosion. Once water levels overtop
118 the marsh platform, forces on the face decrease (Tonelli et al., 2010) and the cliff begins to act to both
119 reflect and shoal waves, with a proportion of the wave energy propagating beyond the margin depending on
120 wave height to water depth ratios (Möller and Spencer, 2002). Under most conditions these landforms do
121 not produce regions of low hydrodynamic energy in front of them at the instantaneous timescale and are
122 therefore principally erosive features which will continue to retreat once formed. Over longer timeframes
123 eroded material may become deposited on the fronting mudflat (hydrodynamic conditions permitting), raising
124 its elevation and increasing energy dissipation. This may gradually lead to sufficient energy absorption to

125 halt cliff retreat and the feature becoming relict (Allen, 1989). Fronting mudflats may also widen through
126 marsh retreat, either enhancing energy dissipation and reducing erosion (Mariotti and Fagherazzi, 2010) or
127 increasing fetch, thereby enhancing wave power and, consequently, erosion (Marani et al., 2011; Mariotti and
128 Fagherazzi, 2013; Leonardi et al., 2016).

129 Ridge-runnel describes a transition type that is of intermediate cross-shore slope but characterised by
130 topographic variability of significant amplitude relative to the elevation change over the transition zone and
131 landforms that are largely shore-normal in alignment. Little work has been done to investigate formation
132 of, and processes within in ridge-runnel systems of saltmarshes. The work of Priestas and Fagherazzi (2011)
133 on similar landforms that they term wave-cut gullies, may provide some insight into the evolution and
134 hydrodynamic processes that form and perpetuate such landforms. The gullies that they study are isolated,
135 whereas ridge-runnel tends to comprise a repeating alongshore pattern of similar structures. Gullies may
136 therefore represent an intermediate morphology between cliff and ridge-runnel. The hydrodynamic effects
137 of (and on) spur and groove morphologies in coral reef systems have, however, been studied for many years
138 (e.g. Roberts et al. (1975, 1992)). Such systems bear striking similarities to ridge runnel landforms, although
139 the scale can be substantially greater. Some inferences regarding hydrodynamic-landform interactions may
140 therefore be drawn from findings in coral reef contexts alongside broader saltmarsh literature. For deep water
141 depths and long wavelengths the ridge-runnel topography may modify the hydrodynamics at the interface in
142 a similar manner to the ramped margin, i.e. relatively uniformly and dissipatively since the topography acts
143 as an enhanced roughness for waves with lengths exceeding the topographic length scale. As water depths
144 decrease, or wave heights increase, the amplitude and wavelengths of the ridge-runnel features will lead to
145 substantially different wave-bed interactions compared to a ramped margin. Recent hydrodynamic modelling
146 in spur and groove systems has shown that the topography drives local circulation cells under conditions
147 where the wavelengths of landform and incoming waves are such that diffraction leads to alongshore variations
148 in wave height (Rogers and Monismith, 2014).

149 The three-dimensional flow fields are likely to be complex with small-scale refraction and reflection
150 processes leading to a high spatial heterogeneity in energy concentration and the vectors of those forces are
151 likely to be less uniformly shore-normal than for a ramp or a cliff, representing a potential feedback that

152 reinforces the landform heterogeneity. During specific points in the tidal cycle flows become channelised
153 in a shore-normal direction, with localised enhanced long-shore flows from ridge to runnel. Erosive and
154 depositional environments may be found in close proximity with a high degree of temporal variability also
155 being apparent.

156 **2 Methods**

157 **2.1 Marginal morphometry and classification**

158 Marsh edge morphologies were investigated on the coastlines of East Anglia, UK (Figure 2). Field ob-
159 servations and aerial photographic interpretation indicate that marsh margins adopt a limited number of
160 characteristic forms within this study region and that they are broadly similar to those observed elsewhere
161 (Allen, 2000), and described above.

162 The marsh margin, defined as the point of transition between vegetated and un-vegetated foreshore,
163 was manually digitised from Environment Agency true colour aerial photography with a pixel size of 25cm,
164 acquired in either summer 2013 (Essex) or summer 2014 (Suffolk and Norfolk) and represented as a polyline.
165 The same marsh margin line was used for the change detection analysis (section 2.2), ensuring co-location
166 of morphometry and change data whilst maintaining methodological comparability. For the purposes of
167 this study the marsh margin, as determined for 2013-2014, was assumed to be adequately representative of
168 the marginal position in 2008 when LiDAR data were acquired. In order to fully automate the workflow,
169 an automated classification allowing for determination of marsh edge location would have been ideal. This
170 challenge is non-trivial, however, and was beyond the scope of this project. The challenges associated with
171 automating this stage of the process, and justifications for using a manual vectorisation approach, are further
172 detailed in the supplementary material.

173 The shoreline vector was then passed to an automated process (in Arc GIS 10.2) to compute mor-
174 phological parameters at the marsh margin based upon composite LiDAR DTM data with 25cm pixel
175 size, acquired in summer 2008 as part of a strategic monitoring programme by the Environment Agency
176 (<http://environment.data.gov.uk/ds/survey>). The initial stages conducted for this analysis are represented

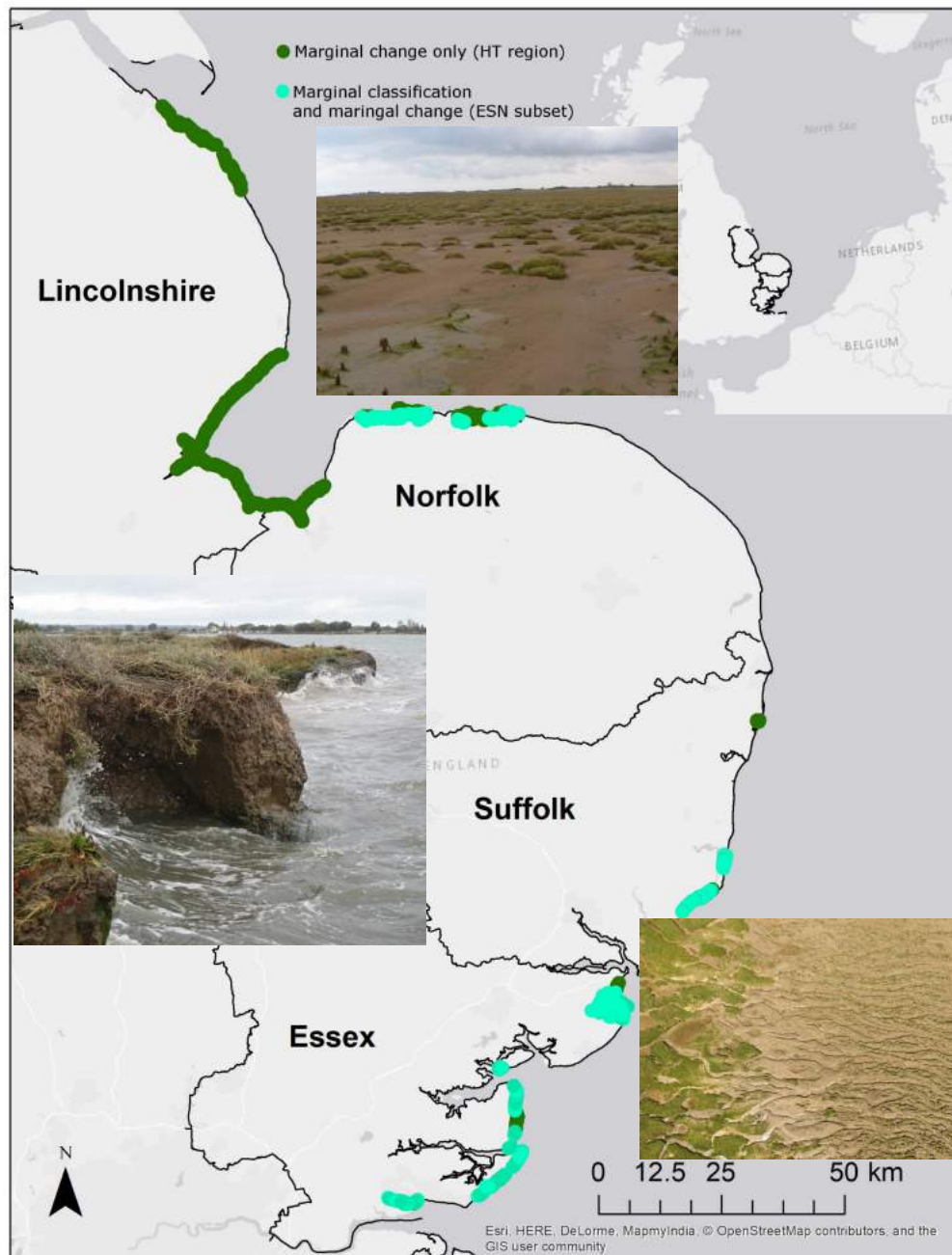


Figure 2: Location of study showing regional coastline of East Anglia comprising four coastal counties (Essex, Suffolk, Norfolk and Lincolnshire). Data coverage upon which analyses are based is indicated, with the parts of the region between The Humber and The Thames for which marginal change estimates were available being denoted HT, and the subset for which it was also possible to classify margin types being denoted ESN. Photo inserts: Top - ramped margin, Lincolnshire (B. Evans), Middle - cliffed margin, Essex (I. Möller), Bottom - ridge-runnel margin, Essex (B. Evans)

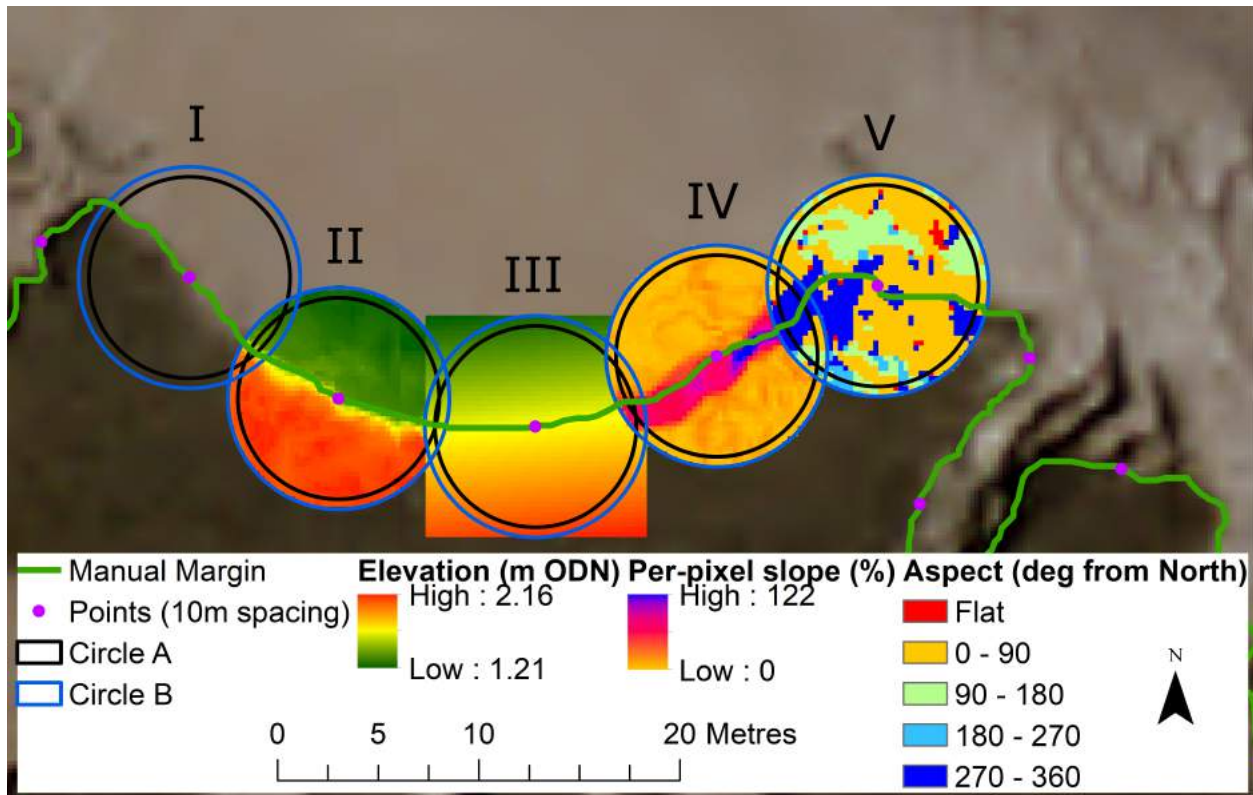


Figure 3: Initial geoprocessing stages for morphometric analysis superimposed upon 2013 aerial photograph of a section of marsh cliff (Essex). Manually-digitised shoreline vector is shown in green, with points established at 10m intervals along it. I=circles A and B, II=LiDAR elevation, III=elevation of first order surface, IV=per-pixel slope and V=per-pixel aspect in degrees from North.

177 in Figure 3. Points were created along the margin polyline, separated by a user-specified step distance that
 178 allows sampling density to be varied according to requirements. In this case a step distance of 10m was used.
 179 A circle of specified radius (10m here, equating to approximately 1250 pixels of the 25cm LiDAR raster)
 180 was then buffered around each point. For each such circle (henceforth "circle A"), a second circle ("circle
 181 B") was defined (I in Figure 3), having a diameter equal to that of the original circle plus four pixel widths
 182 (i.e. +1m for the 25cm DEM - II in Figure 3). This additional buffering avoids edge effects relating to some
 183 treatments of the raster data such as calculation of pixel slope and aspect, which require a full complement
 184 of adjacent pixels.

185 The cross-shore slope of the marginal zone was described by fitting a first order (least-squares) surface
 186 through the DEM for circle B (III in Figure 3) and computing its slope (%) and aspect (to determine
 187 shoreline orientation) within circle A. The shoreline azimuth was taken as perpendicular to the aspect and

188 was used to denote the offshore direction (approximately North in Figure 3).

189 A normalised-difference orientation index (NDMOI) was developed to describe the alignment of marginal
190 landforms relative to the shoreline azimuth. Slope (%) (IV in Figure 3) and aspect (V in Figure 3) relative
191 to the shoreline azimuth (degrees) were computed for each pixel of the LiDAR DTM within Circle A, based
192 on the DEM of circle B. Masks were then computed identifying pixels whose aspect is broadly aligned (± 45
193 degrees) to the shoreline azimuth and those that are broadly perpendicular to it (± 45 degrees of shoreline
194 aspect). Assuming that greater slopes describe more functionally significant topographical variation (in
195 terms of hydrodynamic interactions), the sum of slope values for each class of pixel (aligned ($\Sigma_{S_aligned}$) or
196 perpendicular ($\Sigma_{S_perpendicular}$) was calculated. To provide a stable and readily interpreted index of landform-
197 to-shoreline alignment, a normalised difference transformation was applied to the sums of slopes (Equation 1).
198 The resulting index is in the range -1:1, with positive values indicating a dominance of landform alignment
199 perpendicular to the shoreline (e.g. shore-normal ridge-runnel systems) and negative values indicating a
200 dominance of shore-aligned landforms (e.g. a linear cliff).

$$NDMOI = (\Sigma_{S_aligned} - \Sigma_{S_perpendicular}) / (\Sigma_{S_aligned} + \Sigma_{S_perpendicular}) \quad (1)$$

201 Topographic complexity, amplitude, and the frequency of different magnitudes of elevation change were
202 represented by the kurtosis of the frequency distribution of per-pixel slopes within circle A. In order to remove
203 the confounding influence of variable ranges of slope values over which kurtosis was calculated, frequencies
204 were computed for slopes in the range 0-100% with a bin width of 5%. The bin size and number of bins (and
205 therefore the overall range of slopes considered) were tunable parameters, but 20 bins of width 5% were found
206 to provide good separation between the desired classes. Examples of relevant values, for individual example
207 locations representing each end-member type, are shown in Figure 4. Kurtosis values of the distributions
208 shown in panel C are: ramp=15.73; cliff=0.22 and ridge-runnel=-0.18.

209 For each circle A (ca. 1250 pixels), the process also derived other zonal statistics describing the mor-
210 phology represented by the LiDAR DTM. These included minimum elevation, maximum elevation, elevation
211 range, skewness of the slope distribution and the median absolute difference (Trevisani and Rocca, 2015).
212 Exploratory analysis of the results showed that these supplementary zonal statistics provided little added

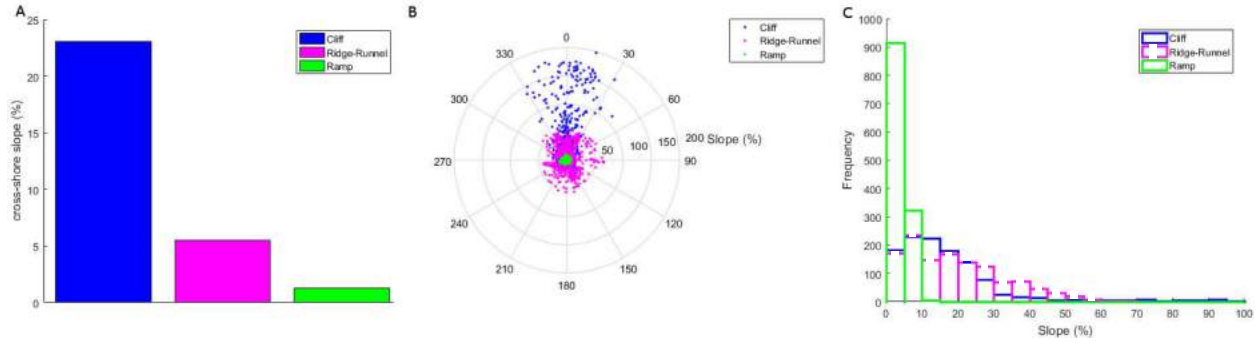


Figure 4: Comparison of margin type indicators for example 10m diameter circles representative of each class based on their position within the parameter space . (A) first-order slope through DEM points. (B) Distribution of per-pixel slopes and aspects relative to shore-aligned (polar axis, 0 degrees). (c) frequency distribution of per-pixel slopes

213 separation between different marginal landform types. Sensitivity tests were conducted to assess the effect of
 214 sampling area on discrimination of these types. The comparison showed that a 10m diameter sampling cir-
 215 cle maximised overall parameter-space separation. Smaller circles suffered from insufficient sampling points
 216 (taken from a 25cm raster) to properly constrain the distribution of between-pixel slopes that described to-
 217 pographic complexity. Smaller circles are also more vulnerable to location errors relative to the topographic
 218 margin arising from the manual digitisation procedure and the temporal mismatch between the imagery
 219 from which margin location was derived and the DEM being sampled. This means that there is a higher
 220 probability of smaller sampling circles not actually sampling the margin but falling either landward or sea-
 221 ward of it. Larger circles resolved differences in cross-shore slope poorly because they incorporated too much
 222 non-marginal (and therefore essentially flat) topography.

223 A three-class unsupervised (k-means) classification of the entire dataset was carried out to objectively
 224 separate the landform types based on their slope, landform alignment and topographic complexity.

225 The classification was applied to marsh margins in Norfolk, Suffolk and Essex at an along-shore spacing
 226 of 10m, resulting in 41449 margin type classifications.

227 For this particular study validation is problematic. No formal typology of margins exists against which an
 228 unequivocal validation could be conducted. While Allen (1993) describes characteristics defining distinctive
 229 margin types, no attempt is made to map or quantify these. There is therefore no 'benchmark' against
 230 which to compare the classifications derived here, and certainly no previous quantitative typology against
 231 which to validate findings. In order to estimate classifier performance, regions were manually identified that

232 were considered, based on field and aerial photographic observations, to be overwhelmingly dominated by
233 a given margin type. Classifications within these regions were assessed. Only one region was deemed to
234 be characterised almost exclusively by ridge-runnel morphology (Tillingham, Essex), coverage of which was
235 limited by lack of LiDAR data for some of the area. Consequently the validation set for ridge runnels was
236 considerably smaller than for the other two classes ($n=47$). A total of 683 classified circles (A) were used for
237 validation. Manually determined margin type was compared to classification outputs. The overall correct
238 rate was 0.82, with a sensitivity (true positives rate) of 0.71 and specificity (true negatives rate) of 0.95.

239 **2.2 Changes in margin position**

240 Lateral marsh morphodynamics were represented by the change in position of the marsh margin over time.
241 The marsh margin was defined as the point of transition from vegetated to un-vegetated substrate. The
242 aim was to achieve the longest possible interval over which to measure change using comparable datasets of
243 similar spatial resolution. The dataset chosen for analysis of marginal position was therefore the Environment
244 Agency aerial photography. The baseline year (t_0) was chosen as the first for which a relatively comprehensive
245 survey of the coastline in question was acquired, namely 1992. The second comparison year (t_1) was chosen
246 as the most recent dataset available at the time the analysis was started. For Essex this was acquired in
247 2013, while for the rest of East Anglia it was 2014. The 1992 imagery was panchromatic with a 25cm pixel,
248 while the 2013/14 imagery was four-band (including infrared) at 20cm resolution.

249 Aerial surveys were conducted in late summer/early autumn and as such represent the period of maximum
250 seasonal growth on the marshes. The transition from vegetated to un-vegetated surfaces is therefore likely
251 to represent the limit of annual rather than perennial vegetation in cases where the shoreline profile is
252 such that these two differ. Manual digitisation of marsh margins based on visual assessment of the aerial
253 photography offered a consistent methodology across datasets of different spectral characteristics and a
254 robust and accurate determination of the position of the marsh margin. Baily and Pearson (2007) opted for
255 a similar methodology when seeking to estimate changes in marsh extent on the South coast of the UK as
256 did McLoughlin et al. (2015) in Virginia, USA.

257 For each year (1992 or 2013/14), the aerial photographs, supplied by the Environment Agency as or-

258 thorectified and colour-balanced images, were imported into ArcMap 10.2 (ESRI) and the marginal position
259 was then digitised using a graphics tablet (UGEE M708). Digitisation was conducted with the imagery
260 zoomed to greater than 1:500 as a compromise between having sufficient contextual information to locate
261 the margin and minimising errors relating to manual precision.

262 Errors related to interpretation of margin location were estimated by repeat digitisation (n=10) of 2.5km
263 long subset regions on different days. Errors related to the precision with which the desired shoreline
264 vector could be drawn were estimated by multiple tracing (n=10) of an existing vector along the same
265 sections. Differences between vectors were calculated at 10m intervals using the 'near' function within ArcGIS.
266 Interpretation errors were found to differ based on margin type and are reported in Table 1. Tracing errors
267 had a root mean square error (RMSE) of 0.27m and coefficient of variation (CoV) of 0.99m. Image co-
268 registration errors were estimated using 62 control points across the region. RMSE was 1.22m and CoV
269 0.83m. No systematic direction of error was identifiable. Errors were found to be highest where margins
270 were most dynamic, which meant that signal-to-noise ratios typically remained low in these locations (see
271 results section).

272 Regional coverage was typically good on the open coast and in outer estuarine areas but poor in inner
273 estuaries such as those of Essex and Suffolk. This introduces a degree of sampling bias by excluding some
274 of the more sheltered and fluviially-affected parts of the marsh system. Creek margins were digitised for
275 creeks exceeding 20m width. Following digitisation of the marsh margins for both time periods, the change
276 in position was estimated using the Digital Shoreline Analysis System (DSAS) (Theiler et al., 2008). DSAS
277 is an extension for ArcGIS that estimates the Shoreline Change Envelope (SCE (m)) and End Point Rate
278 (EPR (my^{-1})) by calculating the intersections of date stamped shorelines with shore-normal transect lines
279 cast from a baseline. DSAS transects were cast at 10m intervals along the baseline and were manually filtered
280 to exclude those approaching the shoreline obliquely ($>45^\circ$) as a result of the high planform complexity of
281 the marsh systems. A total of 33287 shoreline change estimates were thereby derived, covering the coastline
282 between The Humber and The Thames (henceforth referred to as HT - see Figure 2).

283 LiDAR coverage only extended to the marsh margins in Essex, Suffolk and Norfolk and was not com-
284 prehensive within these counties. Margin classifications at 10m intervals were associated with lateral change

285 rates by executing a spatial join between the centrepoint of each DSAS transect (clipped to the SCE) with
286 the nearest centroid of a margin classification circle. A maximum search radius of 20m was used to ensure
287 that only nearby marginal classification data were extracted. Volumetric change rate (VCR) estimates were
288 obtained by combining lateral migration rates with elevation ranges calculated during margin type classifica-
289 tion. Two assumptions were required; that landform types are consistent through the period of observations
290 (McLoughlin et al., 2015) and that elevations in the 10m sampling diameter are representative of the cross-
291 shore range of elevations at the margin. This resulted in a dataset of 15774 paired margin type and change
292 estimates (this subset henceforth referred to as ESN - see Figure 2).

293 **2.3 Exposure of margin**

294 The ESN subset was additionally divided into locations that were exposed and those that were sheltered.
295 The criterion applied was whether the margin location has uninterrupted (by marsh platforms represented
296 in the Phelan et al. (2011) dataset or by land masses) line of sight to any point 10km offshore. 'Exposed' is
297 henceforth used to denote those margins with a line of sight to any point 10km offshore, whilst 'sheltered'
298 denotes those that do not. The analysis was conducted in Arc GIS 10.2 using the 'viewshed' tool.

299 **3 Results**

300 Proportions of margin classes within the ESN subset were 20.1% ramps (n=3166), 48.8% cliffs (n=7705) and
301 31.1% ridge-runnel (n=4903). These were very similar to the overall set of margin classifications, including
302 those not associated with change estimates, for which 20.5% were ramps(n=8507), 46.1% cliffs (n=19100)
303 and 33.4% ridge-runnel (n=13824).

304 Table 2 compares descriptive statistics for marginal change rates across the entire HT regional extent to
305 those for the subset of locations with margin classes (ESN) and the exposed and sheltered locations within
306 the ESN subset. Histograms of all four populations are shown in Figure 5.

307 In Matlab one-way ANOVA followed by a multiple comparison test using the 'multcompare' function was
308 used to test for differences in the mean EPR and VCR between margin classes for the ESN subset. Tests
309 were replicated for the exposed and sheltered locations within ESN. Both signed and absolute quantities for

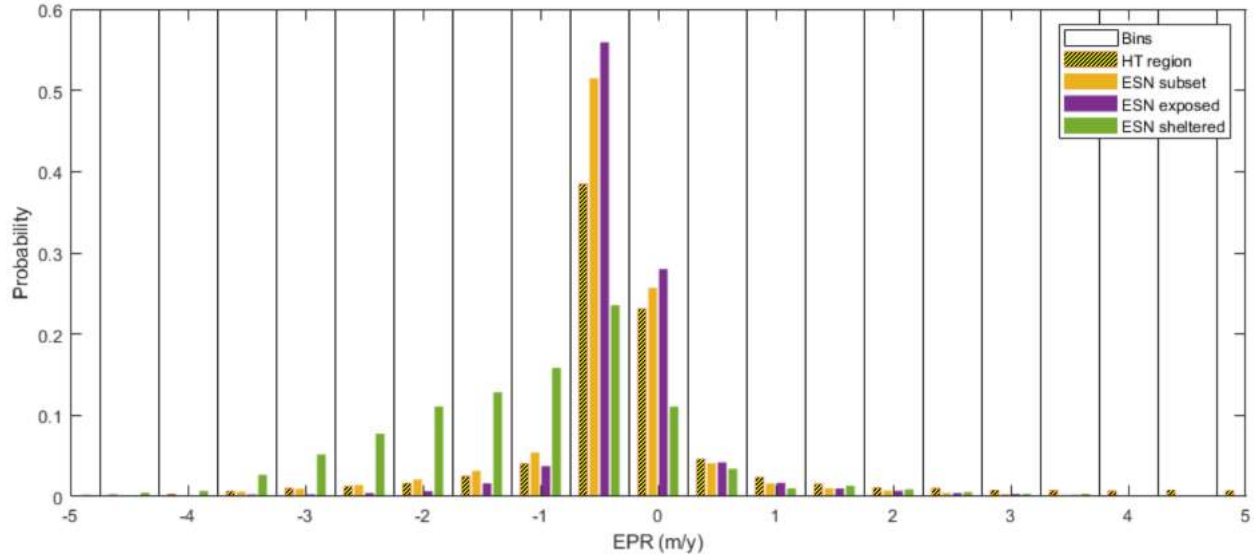


Figure 5: Probability distributions of EPR for entire HT region, ESN subset, Exposed and Sheltered locations within the ESN subset

310 each change metric were tested. The Scheffe procedure was selected as the most conservative option suitable
 311 for unbalanced sample sizes. Results of the multiple comparison tests are presented in Figure 6 and Table 3.

312 3.1 Planimetric changes

313 Over the HT region we find a mean advance of marsh margins by 2.42 m/y, albeit with high variability
 314 (SD 6.85m). In comparison, for ESN only, there is mean retreat at -0.1 m/y (SD 0.88m). Rapid advance of
 315 marsh margins is observed in The Wash embayment, with a maximum rate of progradation of $75.78\text{m}\text{y}^{-1}$.
 316 It is the widespread and rapid vegetation establishment in this area that is responsible, in large part, for
 317 the increased range and standard deviation compared to ESN, and this results in a more positively skewed
 318 and leptokurtic distribution of EPR. The contrast between a maximum retreat of 10.95 m/y and advance
 319 of more than 75 m/y is striking. Both HT and ESN regions show positive skew around medians very close
 320 to zero, which also implies a tendency for advance to outpace retreat. In exposed settings (section 2.3) we
 321 see strong mean retreat but retain positive skewness for all margin types with the notable exception of cliffs.
 322 For sheltered environments the median retreat is again very close to zero and the population is positively
 323 skewed. This implies that cliffs in exposed locations are the only context in which we observe retreat rates
 324 typically to outpace rates of advance.

325 Within the ESN region, all margin types demonstrate a tendency towards retreat, reflecting an overall
326 erosive trend. Results show that, in terms of lateral migration rates, the behaviour of the three classes is
327 significantly different with ramps, on average, retreating fastest (0.23my^{-1}). Cliffs have the lowest lateral
328 retreat rates (EPR, row A in Figure 6), with ridge-runnels exhibiting intermediate behaviour. Ramps retreat
329 with a mean rate approximately two and a half times that of ridge-runnels and nearly five times that of
330 cliffs.

331 For exposed settings EPR becomes strongly negative (erosive) across all margin types with cliffs exhibiting
332 significantly slower retreat than the other two classes. In sheltered conditions ramps and ridge-runnels
333 become slightly accretional on average while cliffs remain very slightly erosional (-0.01my^{-1}). Magnitudes
334 of mean change are an order of magnitude smaller than for exposed contexts. External forcing, in terms of
335 hydrodynamic exposure, therefore appears to be more important than any morphodynamic feedback signal
336 for controlling decadal-scale changes in margin position.

337 When the absolute EPR, a measure of lateral dynamism, is considered (row B in Figure 6) the results
338 show that, over the ca. 20 year time period of change assessed here, ramps are much more dynamic than
339 ridge-runnels which in turn are more dynamic than cliffs. This pattern holds for both exposed and sheltered
340 environments, with all classes being less dynamic when sheltered than the least dynamic class (cliffs) when
341 exposed. Geomorphic context and energy exposure therefore appear to strongly influence the potential for
342 lateral changes observed at marsh margins (Leonardi and Fagherazzi, 2014). This concurs with previous
343 work that has identified a linear relationship between marsh edge retreat and wave power (Marani et al.,
344 2011; Leonardi et al., 2016).

345 **3.2 Volumetric changes**

346 When the signed VCR (row C in Figure 6) is considered, volume changes in cliffs and ridge-runnels are
347 no longer significantly different across ESN, while changes at ramped margins remain separable from, and
348 significantly more negative than, the other classes. This implies that, although the rates of change in margin
349 position may be substantially different between cliffed and ridge-runnel margins, the volumes of sediment
350 exchanged during migration of these landforms are similar. Exposed cliffs become the most volumetrically

351 erosive type, moving significantly more sediment than ramps. Therefore, while they may be apparently
352 the most stable landform in terms of EPR, when exposed to high energy they exhibit the greatest rate
353 of sediment mobilisation (geomorphological work), which confirms previous claims to their efficiency at
354 concentrating energy (e.g. van De Koppel et al. (2005)). Cliffs are also the most erosive features in terms
355 of VCR for sheltered environments, which aligns with their negative EPR. Importantly, sheltered VCR is
356 also negative for ramps and ridge-runnels, despite their EPR being positive. This demonstrates that, in
357 low energy conditions, it is the steeper examples of these landforms that retreat while those with shallower
358 cross-shore slopes tend to prograde.

359 Dynamism, as represented by absolute VCR (row D in Figure 6), appears to be greatest for ramps and
360 smallest for cliffs across the ESN subset. In exposed settings, however, ramps show the lowest dynamism,
361 while volume changes in cliffs and ridge-runnels are substantial (exceeding $1\text{m}^3\text{y}^{-1}$) but very similar between
362 classes. For sheltered regions the mean absolute volumetric changes show no significant differences between
363 any of the margin types.

364 4 Discussion

365 4.1 Distribution of margin types

366 The inventory facilitated by the typology developed here demonstrates that, within the ESN region, margin
367 types are not evenly distributed. Cliffs are the most common type, followed by ridge-runnels, with ramped
368 margins being relatively rare. The relative paucity of ramped margins arises since, as previously noted,
369 planar slopes tend not to persist at marsh margins since vegetation presence or establishment leads to
370 increased topographic complexity (Temmerman et al., 2007). The ramped class, therefore, may not represent
371 a morphodynamically stable condition. The dominance of cliffed margins suggests, in contrast, that these
372 are a relatively stable (persistent) marginal form. The high membership of the class referred to here as ridge-
373 runnel is disproportionate to the presence of these landforms based on visual assessment of the region. This is
374 because the classification includes within this category many relatively isolated areas where the planform of
375 the margin is complex within the 10m scale of the morphometric calculations. Such areas are typically creek

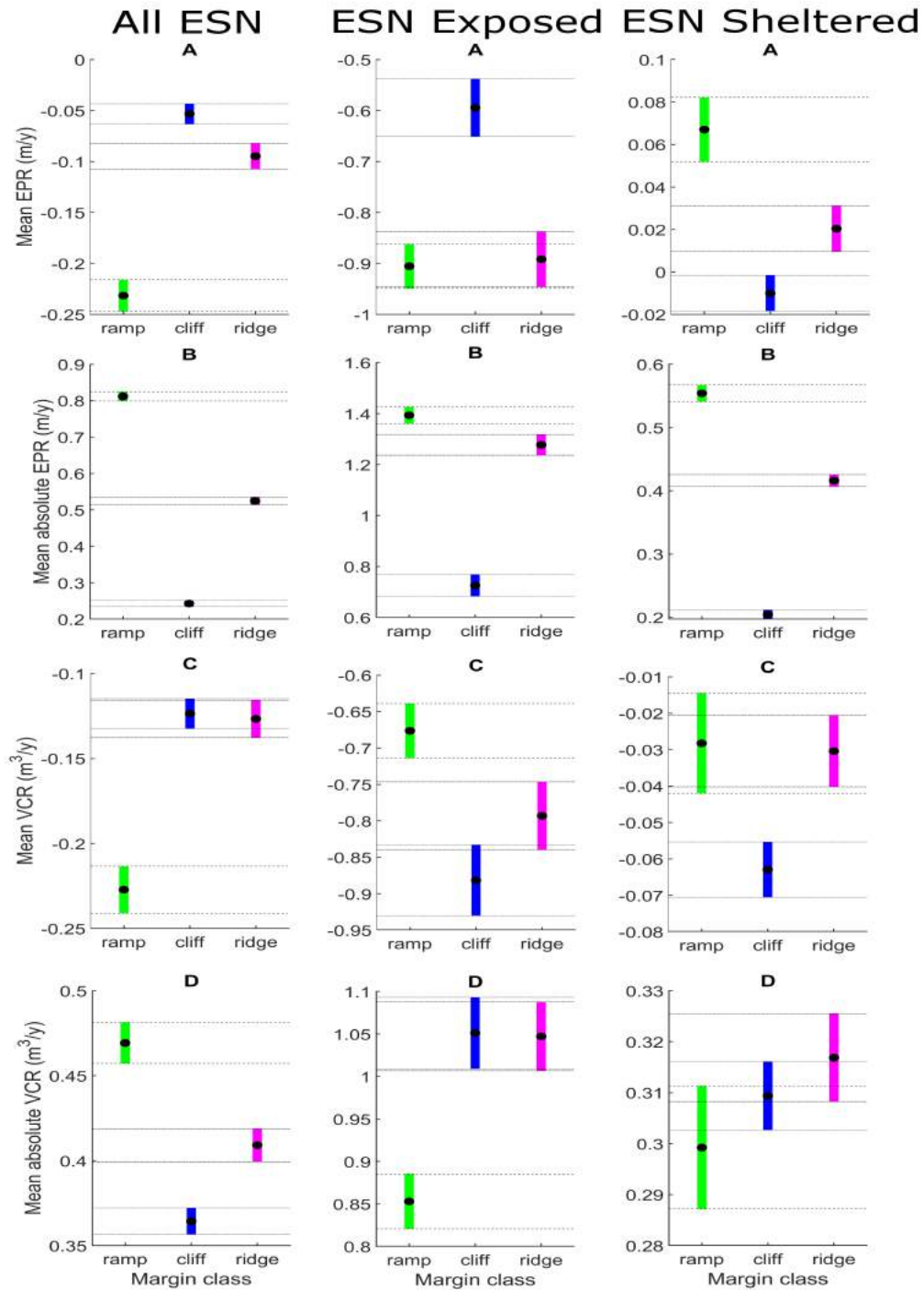


Figure 6: Multiple comparison of mean margin type behaviours for the entire ESN region (top panel) in addition to exposed (middle panel) and sheltered (bottom panel) locations within it. A: EPR, B: Absolute EPR, C: VCR, D: Absolute VCR. Horizontal dashed lines indicate one standard error. Note that y-axis scales vary between panels for clarity. 'ridge' denotes ridge-runnel

376 intersections, abrupt channel meanders or areas where smaller ($\approx 5\text{m}$ wide) creeks are present. Examples of
377 this are visible in Figure 7. The class may also include any wave gullies (Priestas and Fagherazzi, 2011) that
378 are present. Ridge-runnels, if considered as analogous to spur and groove formations in coral reef systems,
379 may be representative of a very sensitive region of the energy continuum and therefore be a rather plastic
380 class in which small variations in energy are reflected in substantial morphological variability (Roberts et al.,
381 1992). Exposed marshes account for only 14% of the margins within the ESN region and margin types are
382 dominated by ramps(45%) and ridge-runnels (29%), with cliffs only comprising 26%. This may represent
383 a tendency for marsh margins in high-energy environments to adopt a more dissipative form, particularly
384 where wave action is of more significance than tidal flows. In sheltered environments (86%), however, cliffs
385 are the most common landform, accounting for 52% of margins. Cliffs with complex planform morphology
386 probably constitute an additional component that is subsumed within the ridge-runnel class, as discussed
387 above. This contrasting landform prevalence between exposed and sheltered locations is likely to arise from
388 the differences in geomorphic setting (wide, flat fronting mudflats in exposed settings compared to narrow,
389 steep mudflats in more constrained channel systems) alongside differences in the balance between wave and
390 tidal energy in terms of hydrodynamic exposure.

391 **4.2 Relationship between margin type and morphodynamics**

392 Overall, the our findings suggest a spatially-variable balance between the importance of external forcing
393 and self-organised controls on landform evolution. Despite a dominance of external factors (exposure) there
394 is clear evidence that margin configuration affects the interactions between landform and hydrodynamic
395 conditions, modulating marsh system responses through time.

396 This study finds that the cliffed condition is a prevalent and probably relatively stable state in sheltered
397 environments whereas its scarcity in exposed areas might suggest that it is a relatively transient landform
398 state where incident energy conditions are higher. The lateral dynamism of these landforms is much less than
399 for other marginal configurations irrespective of exposure, although cliffs do exhibit a greater tendency to
400 be erosional (Mariotti and Fagherazzi, 2010). This, alongside the skewness statistics reported, supports the
401 findings of Gunnell et al. (2013) and the assertion made by Fagherazzi (2013) that marsh advance tends to be

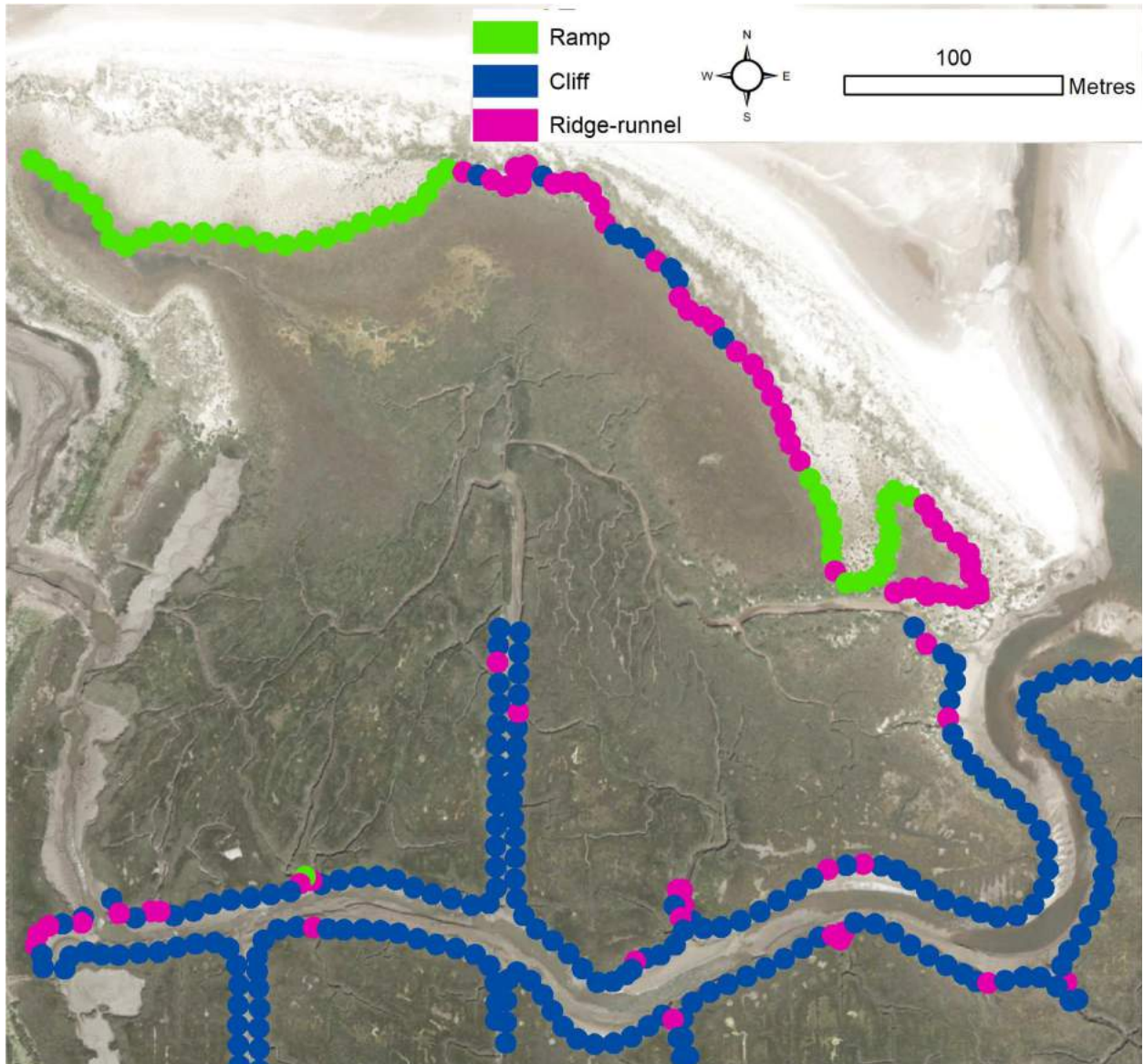


Figure 7: Detail showing aerial photography of a marsh area that exhibits a range of marginal characteristics and their associated classification. Titchwell, North Norfolk. Note the association of ridge-runnel classification with creek junctions and areas of added topographic complexity

402 more rapid than retreat and lends credence to Fagherazzi's assessment of century to millennium timescales
403 for landscape cyclicality. The ensuing conclusion that, over management timescales of decades, changes are
404 likely to be unidirectional is therefore tacitly supported also. The observations of advance associated with
405 some cliffed margins, however, suggests re-establishment of vegetation in front of the scarp, constituting
406 an observation of cyclicality similar to that made by van der Wal et al. (2008) that may also be related to
407 persistence and recolonisation of slump blocks.

408 The finding that advance tends to be faster than retreat contrasts with the behaviour posited by van De
409 Koppel et al. (2005) and Singh Chauhan (2009), in whose models retreat is rapid following criticality in a
410 landform that has prograded gradually. It is possible that these models are appropriate for sandier systems
411 such as Morecambe Bay, but not for the more cohesive East coast systems investigated here (Pringle, 1995).
412 The apparent stability of marsh cliffs is, in part, a consequence of the geomorphic contexts in which they
413 tend to occur. Cliffs dominate the banks of estuaries and channels where tidal flows may be stronger and
414 prevent the accumulation of sediment channelward of the vegetated margin (limiting progradation), while
415 slump blocks may protect the cliffs from erosion (Gabet, 1998; Allen, 2000). In more exposed areas, where
416 mean wave energy is typically greater, landforms (i.e. ridge-runnels) exhibiting greater long-shore variability
417 develop to dissipate the more laterally-variable cross-shore bi-directional currents. Perhaps not surprisingly,
418 these landforms then also exhibit greater variability in morphological change over time.

419 **4.3 Implications of findings**

420 A central question in the development of the marginal classification methodology is that of scale. The
421 relationship between the dimensions of the landscape features that are being measured, the resolution of the
422 data from which measurements are taken and the size of the area over which they are sampled determines
423 the nature and performance of any metrics derived. The empirical observation that a 10m sampling diameter
424 (for a 25cm raster) is most informative of marsh marginal characteristics suggests that 10m is an appropriate
425 scale at which to measure saltmarsh landscape attributes which is commensurate with the dimensions of the
426 features themselves and the scale of their spatial variability. This has implications for future work in terms
427 of desirable grid resolutions for numerical landscape models and also remotely-sensed products. Given the

428 increasing availability of very high resolution topography (e.g. from drones with pixel sizes of less than 1cm)
429 the wider investigation of the influence of data resolution on morphometric indices would be valuable.

430 The findings presented here (particularly the paucity of cliffs in exposed environments) highlight the
431 need for more research to address morphodynamics of other margin types. This is necessary to improve our
432 understanding of their behaviours and hence the future of our marsh systems. We have also demonstrated
433 that geomorphic setting has a significant impact on the nature of observed dynamics for all types of margin.
434 Both empirical studies and numerical models therefore need to represent these contextual considerations
435 much more explicitly than has hitherto been achieved, in order to avoid conflating dissimilar phenomena.
436 Finally, the data presented above show that marginal changes can be very different depending on whether
437 volumetric or lateral metrics are being considered. It is important to understand both types, but inferences
438 made based on lateral dynamics may not necessarily be applicable to volumetric changes and *vice versa*.

439 5 Conclusions

440 This study has demonstrated that salt marsh margin landform types are statistically separable using a small
441 set of indices derived from remotely sensed data. It therefore provides the first quantitative typology for
442 marsh margins of which the authors are aware. Furthermore, the typology is based upon functional differences
443 between landforms that are associated with different morphodynamic and ecosystem service attributes. This
444 is demonstrated by the contrasting morphodynamic behaviours found to be associated with each margin
445 type. We have demonstrated the value of applying quantitative approaches towards the classification of
446 intertidal wetland margins as a means of improving our understanding of their self-organised dynamism,
447 which may form a basis for inferences regarding future morphological change. This study has provided a
448 large sample population across a diverse regional extent, from which it is possible to infer general behavioural
449 tendencies of marsh margins from context and their 3-dimensional functional form. The results presented
450 here therefore provide a robust quantitative basis for a rapid evaluation of likely system dynamism that may
451 be useful to conservation practitioners or site managers.

452 **6 Acknowledgements**

453 We would like to acknowledge the contributions and support of the FAST consortium partners and are
454 grateful for funding to support this work from the European Commission Seventh Framework Programme
455 and the Isaac Newton Trust.

References

- Allen, J. (1989). Evolution of salt-marsh cliffs in muddy and sandy systems: a qualitative comparison of British west-coast estuaries. *Earth Surface Processes and Landforms*, 14:85–92.
- Allen, J. (1993). Muddy alluvial coasts of Britain: field criteria for shoreline position and movement in the recent past. *Proceedings of the Geologists' Association*, 104(4):241–262.
- Allen, J. (2000). Morphodynamics of Holocene salt marshes: a review sketch from the Atlantic and Southern North Sea coasts of Europe. *Quaternary Science Reviews*, 19(12):1155–1231.
- Baily, B. and Pearson, A. (2007). Change Detection Mapping and Analysis of Salt Marsh Areas of Central Southern England from Hurst Castle Spit to Pagham Harbour. *Journal of Coastal Research*, 26(7):1549–1564.
- Balke, T., Stock, M., Jensen, K., Bouma, T. J., and Kleyer, M. (2016). A global analysis of the seaward salt marsh extent: The importance of tidal range. *Water Resources Research*, 52(5):3775–3786.
- Baltz, D. M., Rakocinski, C., and Fleeger, J. W. (1993). Microhabitat use by marsh-edge fishes in a Louisiana estuary. *Environmental Biology of Fishes*, 36(2):109–126.
- Cahoon, D. R. (2006). A review of major storm impacts on coastal wetland elevations. *Estuaries and Coasts*, 29(6):889–898.
- Defina, A., Carniello, L., Fagherazzi, S., and D'Alpaos, L. (2007). Self-organization of shallow basins in tidal flats and salt marshes. *Journal of Geophysical Research*, 112(F3):F03001.
- Dyer, K., Christie, M., and Wright, E. (2000). The classification of intertidal mudflats. *Continental Shelf Research*, 20(10):1039–1060.
- Dyer, K. R. (1998). The typology of intertidal mudflats. *Geological Society, London, Special Publications*, 139(1):11–24.
- Fagherazzi, S. (2013). The ephemeral life of a salt marsh. *Geology*, 41(8):943–944.

479 Fagherazzi, S., Gabet, E. J., and Furbish, D. J. (2004). The effect of bidirectional flow on tidal channel
480 planforms. *Earth Surface Processes and Landforms*, 29(3):295–309.

481 Gabet, E. J. (1998). Lateral Migration and Bank Erosion in a Saltmarsh Tidal Channel in San Francisco
482 Bay, California. *Estuaries*, 21(4):745.

483 Glancy, T. P., Frazer, T. K., Cichra, C. E., and Lindberg, W. J. (2003). Comparative patterns of occupancy
484 by decapod crustaceans in seagrass, oyster, and marsh-edge habitats in a Northeast Gulf of Mexico estuary.
485 *Estuaries*, 26(5):1291–1301.

486 Gray, A., Clarke, R., Warman, B., and Johnson, P. (1989). Prediction of marginal vegetation in a post-
487 barrage environment. Technical report, Institute of Terrestrial Ecology.

488 Gunnell, J. R., Rodriguez, A. B., McKee, B. A., P.M.J., H., D.R., C., S., T., K., S., A., L., and M., B.
489 (2013). How a marsh is built from the bottom up. *Geology*, 41(8):859–862.

490 Leonardi, N., Defne, Z., Ganju, N. K., and Fagherazzi, S. (2016). Salt marsh erosion rates and boundary
491 features in a shallow Bay. *Journal of Geophysical Research: Earth Surface*, 121(10):1861–1875.

492 Leonardi, N. and Fagherazzi, S. (2014). How waves shape salt marshes. *Geology*, 42(10):887–890.

493 Marani, M., Da Lio, C., and D’Alpaos, A. (2013). Vegetation engineers marsh morphology through multiple
494 competing stable states. *Proceedings of the National Academy of Sciences*, 110(9):3259–3263.

495 Marani, M., D’Alpaos, A., Lanzoni, S., and Santalucia, M. (2011). Understanding and predicting wave
496 erosion of marsh edges. *Geophysical Research Letters*, 38(21):n/a–n/a.

497 Mariotti, G. and Fagherazzi, S. (2010). A numerical model for the coupled long-term evolution of salt
498 marshes and tidal flats. *Journal of Geophysical Research*, 115(F1):F01004.

499 Mariotti, G. and Fagherazzi, S. (2013). Critical width of tidal flats triggers marsh collapse in the ab-
500 sence of sea-level rise. *Proceedings of the National Academy of Sciences of the United States of America*,
501 110(14):5353–6.

- 502 McLoughlin, S. M., Wiberg, P. L., Safak, I., and McGlathery, K. J. (2015). Rates and Forcing of Marsh
503 Edge Erosion in a Shallow Coastal Bay. *Estuaries and Coasts*, 38(2):620–638.
- 504 Minello, T. J., Zimmerman, R. J., and Medina, R. (1994). The importance of edge for natant macrofauna
505 in a created salt marsh. *Wetlands*, 14(3):184–198.
- 506 Möller, I. and Spencer, T. (2002). Wave dissipation over macro-tidal saltmarshes : Effects of marsh edge
507 typology and vegetation change. *Journal of Coastal Conservation*, 521(36):506–521.
- 508 Morris, J., Sundareshwar, P., Nietch, C., Kjerfve, B., and Cahoon, D. (2002). Responses of coastal wetlands
509 to rising sea level . *Ecology*, 83(10):2869–2877.
- 510 Phelan, N., Shaw, A., and Baylis, A. (2011). The extent of saltmarsh in England and Wales : 2006 2009.
- 511 Priestas, A. M. and Fagherazzi, S. (2011). Morphology and hydrodynamics of wave-cut gullies. *Geomor-*
512 *phology*, 131(1-2):1–13.
- 513 Pringle, A. (1995). Erosion of a cyclic marsh in Morecambe Bay, northwest England. *Earth Surface Processes*
514 *and Landforms*, 20:387–405.
- 515 Roberts, H., Murray, S., and Suhayda, J. (1975). Physical processes in a fringing reef system. *Journal of*
516 *Marine Research*, 33:233–260.
- 517 Roberts, H. H., Wilson, P. A., and Lugo-Fernández, A. (1992). Biologic and geologic responses to phys-
518 ical processes: examples from modern reef systems of the Caribbean-Atlantic region. *Continental Shelf*
519 *Research*, 12(7):809–834.
- 520 Rogers, J. S. and Monismith, S. G. (2014). Hydrodynamics of spur and groove formations on a coral reef.
521 *Journal of Geophysical Research*, 118(April):145–160.
- 522 Roner, M., Alpaos, A. D., Ghinassi, M., Marani, M., Silvestri, S., and Franceschinis, E. (2016). Spatial
523 variation of salt-marsh organic and inorganic deposition and organic carbon accumulation : Inferences
524 from the Venice lagoon , Italy. *Advances in Water Resources*, 93:276–287.
- 525 Singh Chauhan, P. P. (2009). Autocyclic erosion in tidal marshes. *Geomorphology*, 110(3-4):45–57.

526 Suchrow, S. and Jensen, K. (2010). Plant species responses to an elevational gradient in German North Sea
527 salt marshes. *Wetlands*, 30(4):735–746.

528 Temmerman, S., Bouma, T., Van de Koppel, J., Van der Wal, D., De Vries, M., and Herman, P. (2007).
529 Vegetation causes channel erosion in a tidal landscape. *Geology*, 35(7):631.

530 Theiler, E., Himmelstoss, E., Zichichi, J., and Ergul, A. (2008). Digital Shoreline Analysis System (DSAS)
531 version 4.0 An ArcGIS extension for calculating shoreline change: U.S. Geological Survey Open-File Report
532 2008-1278. Technical report, USGS.

533 Tonelli, M., Fagherazzi, S., and Petti, M. (2010). Modeling wave impact on salt marsh boundaries. *Journal*
534 *of Geophysical Research*, 115(C9):C09028.

535 Townend, I. H. (2008). Hypsometry of estuaries, creeks and breached sea wall sites. *Proceedings of the ICE*
536 *- Maritime Engineering*, 161(1):23–32.

537 Trevisani, S. and Rocca, M. (2015). MAD: robust image texture analysis for applications in high resolution
538 geomorphometry. *Computers & Geosciences*, 81:78–92.

539 van de Koppel, J., Bouma, T. J., and Herman, P. M. J. (2012). The influence of local- and landscape-scale
540 processes on spatial self-organization in estuarine ecosystems. *The Journal of experimental biology*, 215(Pt
541 6):962–7.

542 van De Koppel, J., van der Wal, D., Bakker, J. P., and Herman, P. M. J. (2005). Self-Organization and
543 Vegetation Collapse in Salt Marsh Ecosystems. *The American Naturalist*, 165(1):E1–E12.

544 van der Wal, D., Wielemaker-Van den Dool, A., and Herman, P. M. (2008). Spatial patterns, rates and
545 mechanisms of saltmarsh cycles (Westerschelde, The Netherlands). *Estuarine, Coastal and Shelf Science*,
546 76(2):357–368.

547 Whaley, S. D. and Minello, T. J. (2002). The distribution of benthic infauna of a Texas salt marsh in relation
548 to the marsh edge. *Wetlands*, 22(4):753–766.

Margin type	mean RMSE (m)	range (m)	CoV
Ridge-runnel	4.03	1.45	0.10
Cliff	0.54	0.09	0.06
Ramp	1.18	0.21	0.06

Table 1: Errors associated with identification and manual tracing of marsh margin locations based on panchromatic imagery

Type	Min	Max	Median	Mean	St. Dev	Skew	Kurt	n
HT								
All	-10.95	75.78	0.00	2.42	6.85	3.74	22.78	33287
ESN								
All	-6.10	9.30	-0.05	-0.10	0.88	0.77	16.49	15774
Ramp	-5.71	7.05	-0.08	-0.23	1.25	0.37	7.00	3166
Cliff	-5.40	8.05	-0.04	-0.04	0.55	1.10	40.15	7705
Ridge	-6.10	9.30	-0.07	-0.09	0.99	1.27	15.40	
ESN Exposed								
All	-5.41	9.30	-0.70	-0.82	1.36	0.96	8.30	2162
Ramp	-5.41	7.05	-1.01	-0.91	1.51	1.24	7.46	972
Cliff	-5.40	4.82	-0.35	-0.59	0.95	-1.11	7.51	571
Ridge	-5.11	9.30	-0.82	-0.89	1.41	1.21	9.21	619
ESN sheltered								
All	-6.10	9.07	-0.04	0.01	0.71	2.06	25.98	13612
Ramp	-5.71	5.57	-0.04	0.07	0.99	0.47	9.64	2194
Cliff	-4.99	8.05	-0.04	-0.01	0.47	3.49	59.43	7134
Ridge	-6.10	9.07	-0.05	0.02	0.85	2.29	21.31	4284

Table 2: Descriptive statistics for EPR (m y^{-1}) calculated across entire HT region, for ESN locations where paired margin classifications and change estimates are available, and sub-divided into exposed and sheltered ESN locations. St. Dev = Standard deviation, Skew = skewness, Kurt = Kurtosis, 'Ridge' denotes ridge-runnel

Class (i)	Class (ii)	95% CI LB	Diff (means)	95% CI UB	p-Value
All ESN					
EPR					
ramp	cliff	-0.223	-0.178	-0.133	<0.001
ramp	ridge	-0.186	-0.137	-0.088	<0.001
cliff	ridge	0.002	0.041	0.081	0.034
Absolute EPR					
ramp	cliff	0.531	0.569	0.606	<0.001
ramp	ridge	0.246	0.287	0.328	<0.001
cliff	ridge	-0.315	-0.282	-0.249	<0.001
VCR					
ramp	cliff	-0.144	-0.104	-0.063	<0.001
ramp	ridge	-0.144	-0.101	-0.057	<0.001
cliff	ridge	-0.032	0.003	0.038	0.977
Absolute VCR					
ramp	cliff	0.070	0.105	0.140	<0.001
ramp	ridge	0.022	0.060	0.098	<0.001
cliff	ridge	-0.075	-0.045	-0.014	0.002
ESN Exposed					
EPR					
ramp	cliff	-0.486	-0.311	-0.136	<0.001
ramp	ridge	-0.184	-0.014	0.157	0.981
cliff	ridge	0.105	0.297	0.489	<0.001
Absolute EPR					
ramp	cliff	0.536	0.668	0.799	<0.001
ramp	ridge	-0.012	0.116	0.244	0.086
cliff	ridge	-0.696	-0.552	-0.407	<0.001
VCR					
ramp	cliff	0.055	0.206	0.355	0.004
ramp	ridge	-0.030	0.117	0.263	0.149
cliff	ridge	-0.253	-0.088	0.077	0.423
Absolute VCR					
ramp	cliff	-0.328	-0.198	-0.068	<0.001
ramp	ridge	-0.321	-0.194	-0.068	<0.001
cliff	ridge	-0.139	0.004	0.147	0.998
ESN Sheltered					
EPR					
ramp	cliff	0.035	0.077	0.119	<0.001
ramp	ridge	0.001	0.047	0.092	0.043
cliff	ridge	-0.64	-0.030	0.003	0.086
Absolute EPR					
ramp	cliff	0.313	0.350	0.387	<0.001
ramp	ridge	0.098	0.138	0.178	<0.001
cliff	ridge	-0.241	-0.212	-0.183	<0.001
VCR					
ramp	cliff	-0.004	0.035	0.073	0.087
ramp	ridge	-0.039	0.002	0.043	0.992
cliff	ridge	-0.063	-0.033	-0.002	0.032
Absolute VCR					
ramp	cliff	-0.044	-0.010	0.024	0.763
ramp	ridge	-0.054	-0.018	0.019	0.493
cliff	ridge	-0.034	-0.007	0.019	0.790

Table 3: Results of multiple comparison analysis for difference in means of EPR, absolute EPR, VCR and absolute VCR between margin classes with lower (LB) and upper (UB) bounds of the 95% confidence interval and associated p-values for pairwise tests. 'ridge' denotes ridge-runnel. Rows with significant differences at the 5% level are highlighted yellow